CHIN. PHYS. LETT. Vol. 36, No. 7 (2019) 073701

Secular Motion Frequencies of $^{9}Be^{+}$ Ions and $^{40}Ca^{+}$ Ions in Bi-component Coulomb Crystals *

Hai-Xia Li(李海霞)[1,2], Min Li(李敏)[1,2], Qian-Yu Zhang(张乾煜)[1,2], Xin Tong(童昕)[1**]

[1] *State Key Laboratory of Magnetic Resonance and Atomic and Molecular Physics, Wuhan Institute of Physics and Mathematics, Chinese Academy of Sciences, Wuhan 430071*
[2] *University of Chinese Academy of Sciences, Beijing 100049*

(Received 17 April 2019)

We obtain bi-component Coulomb crystals using laser-cooled $^{40}Ca^{+}$ ions to sympathetically cool $^{9}Be^{+}$ ions in a linear Paul trap. The shell structures of the bi-component Coulomb crystals are investigated. The secular motion frequencies of the two different ions are determined and compared with those in the single-component Coulomb crystals. In the radial direction, the resonant motion frequencies of the two ionic species shift toward each other due to the strong motion coupling in the ion trap. In the axial direction, the motion frequency of the laser-cooled $^{40}Ca^{+}$ is impervious to the sympathetically cooled $^{9}Be^{+}$ ions because the spatially separation of the two different ionic species leads to the weak motion coupling in the axial direction.

PACS: 37.10.Ty, 37.10.Rs, 64.70.kp DOI: 10.1088/0256-307X/36/7/073701

Trapped ions, when sufficiently laser cooled, form spatially ordered structures named Coulomb crystals.[1,2] The condition of Coulomb crystallization is that the ratio of the averaged Coulomb interaction energy of neighboring particles to the averaged thermal energy is greater than 175.[3,4] Since only ions with simple level schemes accessible to laser frequencies can be laser cooled directly,[5,6] most atomic ions with complex level structures and molecules ions with ro-vibrational degrees of freedom cannot be laser-cooled directly. Over the past 20 years, laser-cooled ions have been used to cool other ions through the mutual Coulomb interaction in an ion trap. This method of cooling atomic or molecular ions is called sympathetic cooling and has been established as a powerful and convenient technique to produce many trapped, cold atomic and molecular ionic species, generating bi-component or multi-component Coulomb crystals. Until now, several researchers have reported and investigated the sympathetic cooling,[7,8] the typically achieved translational temperatures of the sympathetically cooled ions are from 10 to 100 mK in ion traps.[9–12] It is possible to observe the spatially localized ions, manipulated and addressed on the single particle level, so that they are readily available to a wide range of fascinating applications of precision measurements, such as high-resolution spectroscopies,[13,14] chemical reactions[15–17] and mass spectrometry.[18–20]

The accuracy of the mass spectrometry based on a linear ion trap is closely related to the determination of secular motion frequencies of trapped ions. The effective potentials and secular motion frequencies of the radial and axial directions can be expressed as[21]

$$\Phi_r(r) = \frac{1}{2}M\omega_r^2 r^2, \quad \omega_r^2 = \frac{\kappa_r^2 Q^2 U_{\rm rf}^2}{2M^2 r_0^4 \Omega_{\rm rf}^2} - \frac{\kappa_z Q U_{\rm end}}{M z_0^2}, \tag{1}$$

$$\Phi_z(z) = \frac{1}{2}M\omega_z^2 z^2, \quad \omega_z^2 = \frac{2\kappa_z Q U_{\rm end}}{M z_0^2}, \tag{2}$$

where κ_r and κ_z represent the geometry parameters of the linear trap in the radial and axial directions, ω_r and ω_z are the angular frequencies of the secular motions in the radial and axial directions, respectively, Q and M are the charge and mass of the trapped ions, $2z_0$ is the distance between the end-caps of the linear Paul trap, $2r_0$ is the distance between two diagonal electrodes, $U_{\rm rf}$ and $\Omega_{\rm rf}(f_{\rm rf} \times 2\pi)$ are the amplitude and the angular frequency of an rf trapping field, respectively. In the direction along the axis, the ions are confined by static potentials $U_{\rm end}$ applied to the end-cap electrodes of the trap. The above formulas (1) and (2) are suitable for the study of single component crystals or multi-species ions with very weak coupling in an ion trap.[16,17]

In this work, we obtain strong coupled bi-component Coulomb crystals containing both $^{40}Ca^{+}$ ions and $^{9}Be^{+}$ ions. The secular motion of the two different species of ions in different directions are detected in both the axial and radial directions. The reasons for their secular frequency shifts compared to the single-component Coulomb crystals are discussed.

The configuration of the linear Paul trap used in this experiment was described in detail previously[22] and is discussed only briefly here. The trap consists of four parallel steel rods, each axially partitioned into three sections. The distance between two diagonal electrodes is $2r_0 = 7$ mm, and the distance between the end-caps is $2z_0 = 6.4$ mm. The $^{40}Ca^{+}$ ions are trapped and Doppler cooled by a 397 nm diode laser with an 866 nm repump diode laser. A Coulomb crystal of pure $^{40}Ca^{+}$ ions was observed by a CMOS camera as shown in Fig. 1(a). Subsequently, beryllium atoms are evaporated from a heated atomic oven and ionized by a 355 nm pulsed laser beam to generate beryllium ions $^{9}Be^{+}$. Once the beryllium ions are captured by the ion trap and sympathetically cooled by laser-cooled $^{40}Ca^{+}$ ions, the dark core in the central region of the $^{40}Ca^{+}$ Coulomb crystal appears and

*Supported by the National Natural Science Foundation of China under Grant Nos 91636216, 11504410 and 11474317, and the Strategic Priority Research Program (B) of the Chinese Academy of Sciences under Grant No XDB21020200.
**Corresponding author. Email: tongxin@wipm.ac.cn
© 2019 Chinese Physical Society and IOP Publishing Ltd

expands. By controlling the duration of the ionization laser, bi-component Coulomb crystals containing different numbers of $^{9}Be^{+}$ ions are obtained as shown in Figs. 1(b)–1(e). The density of ions of type i ions, given by the formula $\rho_i = \varepsilon_0 U_{rf}^2 / M r_0^4 \Omega_{rf}^2$.[23] The number densities of $^{9}Be^{+}$ ions and $^{40}Ca^{+}$ ions in the Coulomb crystals shown in Fig. 1 are $2.95(6)\times10^{8}/cm^{3}$ and $6.65(15)\times10^{7}/cm^{3}$, respectively. The errors of densities are determined by the uncertainties of U_{rf}, Ω_{rf} and r_0. The volume of spatial occupation of $^{9}Be^{+}$ or $^{40}Ca^{+}$ ions can be measured from the obtained images, so that the numbers of $^{9}Be^{+}$ and $^{40}Ca^{+}$ ions in a bi-component crystal can be determined. In Figs. 1(a)–1(e), the numbers of $^{40}Ca^{+}$ ions remain the same, N_{Ca} is 852(56). The numbers of $^{9}Be^{+}$ ions, N_{Be}, are 31(2) in Fig. 1(b), 143(10) in Fig. 1(c), 201(14) in Fig. 1(d) and 492(33) in Fig. 1(e). The errors in the ion quantities are due to the inaccuracy of measurements of the Coulomb crystal volumes.

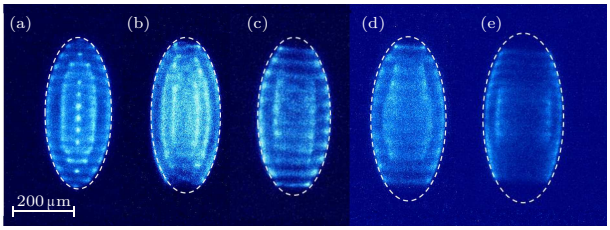

Fig. 1. (a) An image of a pure $^{40}Ca^{+}$ Coulomb crystal. (b)–(e) Four images of $^{40}Ca^{+}$–$^{9}Be^{+}$ Coulomb crystals contain different numbers of $^{9}Be^{+}$ ions under the same trapping condition of $\Omega_{rf} = 2\pi \times 3.2$ MHz, $U_{rf} = 174$ V, $U_{end} = 2.5$ V. The exposure time of the CMOS camera is set to be 2 s for all images. Because of the different contrasts of the images, the brightness is different for different images.

We observed complete spatial separation between the two ionic species. Because of the mass dependence of the radial potential shown in formulas (1) and (2), the axial trapping potentials for two ionic species are the same, whereas the lighter ions $^{9}Be^{+}$ are confined radially more strongly than the heavier ions $^{40}Ca^{+}$ in a linear Paul trap. In addition, the $^{9}Be^{+}$ ions do not fluoresce under the illumination of the $^{40}Ca^{+}$ cooling lasers. Therefore, the $^{9}Be^{+}$ ions appear to occupy the central dark zone and the $^{40}Ca^{+}$ ions surround the $^{9}Be^{+}$ ions forming a bi-component Coulomb crystal with the shell structure.

To obtain the secular motion frequencies in both the radial or axial directions of the trapped $^{9}Be^{+}$ and $^{40}Ca^{+}$ ions, an electric excitation ac field (alternating current) is directed transverse or parallel to the trap axis and superimposed to the trapping fields.[22] When the frequency of the ac field is on resonance with the ion's motion frequency, the excited field pumps energy into the crystal, resulting in the heating of ions and reduction of fluorescence from $^{40}Ca^{+}$ ions. In Fig. 2, two peaks of reduction of fluorescence at 133 kHz and 598 kHz are observed while scanning the frequency of excitation field in the radial direction. They indicate the resonance frequencies of $^{40}Ca^{+}$ and $^{9}Be^{+}$ions in the bi-component Coulomb crystal as shown in Fig. 1(e). According to formula (1), the frequencies for pure $^{40}Ca^{+}$ and $^{9}Be^{+}$ ions are calculated to be 126 kHz and 628 kHz, respectively, under the same trapping condition. Due to the strong motion coupling between the two ionic species in the radial direction, both the resonant frequencies are shifted toward each other compared to the above calculated frequencies.

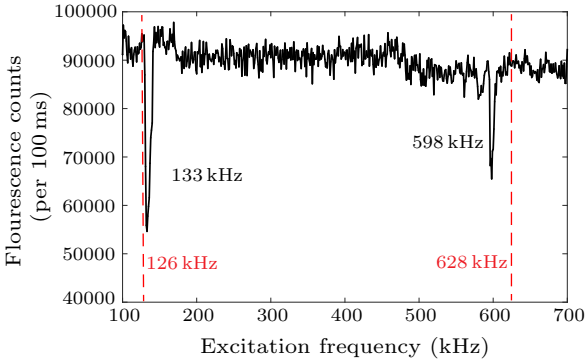

Fig. 2. The change of the fluorescence of the $^{40}Ca^{+}$ ions via the scanning of the ac frequency. The trapping potential settings: $f_{rf} = 3.90$ MHz, $U_{rf} = 174$ V, $U_{end} = 2.50$ V. The red dashed line is the calculated secular motion frequencies of pure $^{40}Ca^{+}$ and $^{9}Be^{+}$ Coulomb crystals.

Under the varied trapping frequency of f_{rf}, the radial secular frequencies of both $^{40}Ca^{+}$ and $^{9}Be^{+}$ ions in four Coulomb crystals (as shown in Figs. 1(b)–1(e)) are measured.

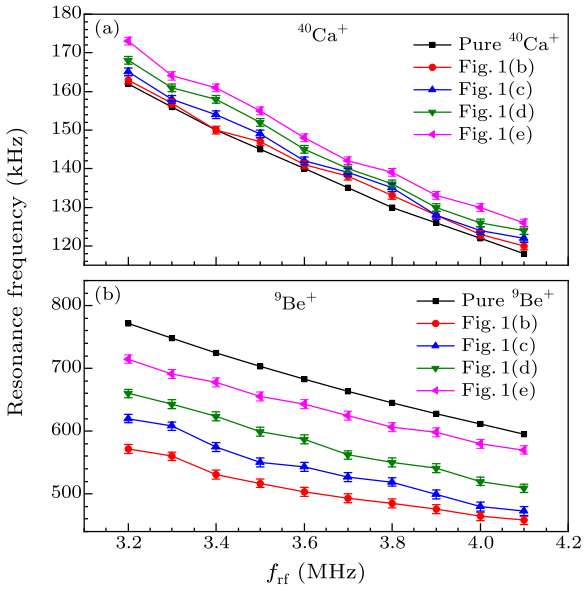

Fig. 3. The radial resonance frequencies of $^{40}Ca^{+}$ ions and $^{9}Be^{+}$ ions in different Coulomb crystals. (a) The radial resonance frequencies of $^{40}Ca^{+}$ ions versus trapping frequency f_{rf}. (b) The radial resonance frequencies of $^{9}Be^{+}$ ions versus trapping frequency f_{rf}. The black lines indicate the theoretical radial secular frequencies of pure $^{40}Ca^{+}$ or pure $^{9}Be^{+}$ ions. The red, blue, green and pink lines stand for the different number ratios of $^{9}Be^{+}$ ions and $^{40}Ca^{+}$ ions in different Coulomb crystals shown in Figs. 1(b)–1(e), respectively. The error bar is the uncertainties of measured resonance frequencies.

The results shown in Fig. 3 indicate that all the measured secular frequencies of $^{40}Ca^{+}$ and $^{9}Be^{+}$ decrease with the increase of the confinement ac frequency f_{rf}, which are in line with the theoretical predication. In a $^{40}Ca^{+}/^{9}Be^{+}$ bi-component Coulomb crystal, when increasing the number of $^{9}Be^{+}$ ions, the

measured secular frequencies of $^{40}Ca^{+}$ ions in radical direction increase and deviate further away from the theoretical frequencies. The measured secular frequencies of $^{9}Be^{+}$ ions in the radial direction, however, get closer to the theoretical predictions. Furthermore, no significant difference of the amount of frequency shift is found for one ionic species in a bi-component Coulomb crystal with different trapping frequencies $f_{\rm rf}$. This indicates that the trapping potential has a slight contribution to the relative frequency shift from a single component Coulomb crystal, and the shift of secular frequency is mainly determined by the ratio of the numbers of two different ionic species.

The axial secular frequencies of the two species ions in the four bi-component Coulomb crystals (as shown in Figs. 1(b)–1(e)) are also measured with the varied end-cap voltage, $U_{\rm end}$. The results are shown in Fig. 4.

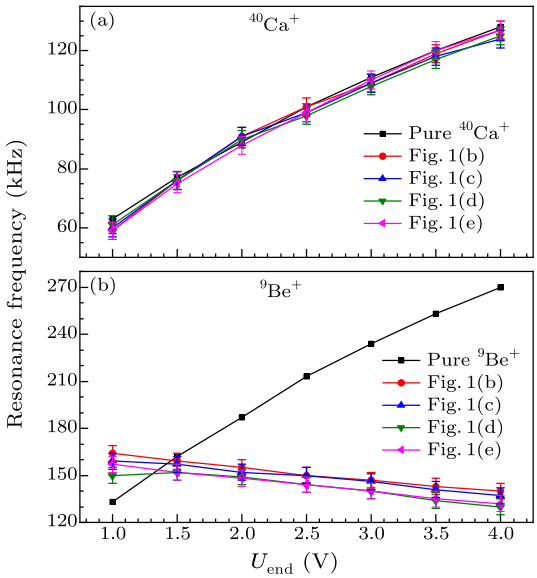

Fig. 4. The axial resonance frequencies of $^{40}Ca^{+}$ ions and $^{9}Be^{+}$ ions in different Coulomb crystals. (a) The axial resonance frequencies of $^{40}Ca^{+}$ ions versus $U_{\rm end}$. (b) The axial resonance frequencies of $^{9}Be^{+}$ ions versus $U_{\rm end}$. The black lines indicate the theoretical axial secular frequencies of pure $^{40}Ca^{+}$ or pure $^{9}Be^{+}$ ions. The red, blue, green and pink lines stand for different number ratios of $^{9}Be^{+}$ ions and $^{40}Ca^{+}$ ions in bi-component Coulomb crystals shown in Figs. 1(b)–1(e), respectively. The error bars are the uncertainties of measured resonance frequencies.

The axial secular frequencies of $^{40}Ca^{+}$ ions in different Coulomb crystals remain almost the same (Fig. 4(a)). They are not affected by the attendance of $^{9}Be^{+}$ ions because the motion coupling in the axial direction between $^{40}Ca^{+}$ and $^{9}Be^{+}$ is weak. In Fig. 4(b), compared with the calculated results for a pure $^{9}Be^{+}$ Coulomb crystal (black line), the measured axial secular frequencies of $^{9}Be^{+}$ ions remain almost unchanged, the small decease may be due to the increased inharmonicity of the electrostatic potential when increasing the end-cap voltage $U_{\rm end}$. When $^{9}Be^{+}$ ions resonate with the excitation ac field, due to the weak motion coupling between $^{40}Ca^{+}$ and $^{9}Be^{+}$ ions in the axial direction, the motion of $^{40}Ca^{+}$ ions is not affected by the motion of $^{9}Be^{+}$ ions. Therefore, unlike in the radial direction, the monitored fluorescence change of $^{40}Ca^{+}$ ions cannot reflect the $^{9}Be^{+}$ resonance frequency in the axial direction of a linear Paul ion trap.

In summary, we have achieved the $^{9}Be^{+}$–$^{40}Ca^{+}$ bi-component Coulomb crystals in a linear Paul trap. The bi-component Coulomb crystal displays a shell structure and encloses an inner dark core, originating from the $^{9}Be^{+}$ ions having a lower mass-to-charge ratio than $^{40}Ca^{+}$ ions. Unlike a single-species Coulomb crystal, the secular motion frequency of ions in a bi-component Coulomb crystal does not fit in with the harmonic potential mode due to the motional coupling between different ionic species. In the radial direction, the motion resonant frequencies of two ionic species shift toward each other. Further detailed studies of motion coupling are required for quantitatively analyzing the shift of motion frequencies for both the ionic species. In the axial direction, the motion frequency of $^{40}Ca^{+}$ ions is almost unaffected by $^{9}Be^{+}$ ions, while the measured motion frequency of $^{9}Be^{+}$ ions deviates greatly from the theoretical frequency. Thus, the motion frequency of $^{9}Be^{+}$ ions cannot be measured accurately with the current method. For a large bi-component Coulomb crystal with a shell structure, the axial motion frequency is not suitable to identify the sympathetically cooled ionic species because of the very weak motion coupling between different ions.

We thank Pan Yong and Zhao Pei for the early work on this project.

References

[1] Raizen M G et al 1992 *Phys. Rev. A* **45** 6493
[2] Drewsen M et al 1998 *Phys. Rev. Lett.* **81** 2878
[3] Pollock E L and Hansen J P 1973 *Phys. Rev. A* **8** 3110
[4] Slattery W L et al 1980 *Phys. Rev. A* **21** 2087
[5] Okada K et al 2007 *Phys. Rev. A* **75** 033409
[6] Zhao X Z et al 2006 *Phys. Rev. A* **73** 033412
[7] Groot-Berning K et al 2019 *Phys. Rev. A* **99** 023420
[8] Chen J S et al 2017 *Phys. Rev. Lett.* **118** 053002
[9] Wübbena J B et al 2012 *Phys. Rev. A* **85** 043412
[10] Kimura N et al 2011 *Phys. Rev. A* **83** 033422
[11] Ostendorf A, Zhang C B, Wilson M A, Offenberg D, Roth B and Schiller S 2006 *Phys. Rev. Lett.* **97** 243005
[12] Meir Z, Pinkas M, Sikorsky T, Ben-shlomi R, Akerman N and Ozeri R 2018 *Phys. Rev. Lett.* **121** 053402
[13] Tong X, Winney A H and Willitsch S 2010 *Phys. Rev. Lett.* **105** 143001
[14] Alighanbari S, Hansen M G, Korobov V I and Schiller S 2018 *Nat. Phys.* **14** 555
[15] Tong X, Wild D and Willitsch S 2011 *Phys. Rev. A* **83** 023415
[16] Baba T and Waki L 2002 *J. Chem. Phys.* **116** 1858
[17] Kas M, Loreau J, Liévin J and Vaeck N 2017 *J. Chem. Phys.* **146** 194309
[18] Schneider C, Schowalter S J, Chen K, Sullivan S T and Hudson E R 2014 *Phys. Rev. Appl.* **2** 034013
[19] Deb N, Pollum L L, Smith A D, Keller M, Rennick C J, Heazlewood B R and Softley T P 2015 *Phys. Rev. A* **91** 033408
[20] Matthey T, Hansen J P and Drewsen M 2003 *Phys. Rev. Lett.* **91** 165001
[21] Berkel D J, Miller J D, Bergquist J C, Itano W M and Wineland D J 1998 *J. Appl. Phys.* **83** 5025
[22] Li H X, Zhang Y, He S G and Tong X 2019 *Chin. J. Phys.* **60** 61
[23] Du L J, Song H F, Li H X, Chen S L, Chen T, Sun H Y, Huang Y, Tong X, Guan H and Gao K L 2015 *Chin. Phys. B* **24** 113703